

Supplementary Information for

Primary cilia and the reciprocal activation of AKT and SMAD2/3 regulate stretch-induced autophagy in trabecular meshwork cells.

Myoung Sup Shim, April Nettlesheim, Angela Dixon, Paloma B. Liton^{a*}

Paloma B. Liton

Email: paloma.liton@duke.edu

This PDF file includes:

- Supplementary Materials and Methods
- Figures S1 to S7
- Table S1
- Legends for Movies S1 to S4
- SI References

Other supplementary materials for this manuscript include the following:

- Movies S1 to S4

Supplementary Materials and Methods

Reagents.

Chemicals and other materials were obtained from the following sources: Chloral hydrate (CH, C8383), cyclopamine hydrate (C4116), dynasore hydrate (D7693), amiloride hydrochloride hydrate (A7410), amlodipine besylate (A5605), NBQX disodium hydrate (N183) DMSO (D2650), bovine serum albumin (BSA; A7906) from MilliporeSigma; SC66 (4398) from Tocris Bioscience; DQ-BSA; SAG (11914), HC067047 (20927), ionomycin (10004974), LY2109761 (15409), SB431542 (13031), from Cayman chemical; phosphate-buffered saline (PBS, 10X; Corning, 46-013-CM); povidone-iodine solution (betadine; 3955-16) from , Ricca Chemical Company; TGF β 2 (T2815) from Sigma-Aldrich; Dulbecco's modified eagle medium (DMEM; 11885084), Dulbecco's PBS (DPBS; 14190235), 100 \times penicillin–streptomycin (Pen/Strep; 15240062), 100 \times penicillin-streptomycin-glutamine (10378016), fetal bovine serum (FBS; 10082147), non-essential amino acids (11140050), gentamycin (15750060), Hank's Balanced Salt Solution (HBSS; 14025092), Lipofectamine® RNAiMAX Reagent (13778075), DAPI (62248), super signal west femto chemiluminescent substrates (34096), DQ™ Red BSA (D12051) from Thermo Fisher Scientific; ECL western blotting detection reagent (RPN2106) from GE Healthcare ; protein size marker (161-0373), protein assay dye reagent concentrate (5000006) and polyvinylidene fluoride (PVDF) membrane for protein blotting (1620177) from Bio-Rad.

Microarrays analysis.

Five micrograms of total RNA from human TM primary cultures with transient silenced autophagy and controls and/or NS and CMS were independently hybridized to human Clariom D microarrays (ThermoFisher) following the manufacturer's instructions at the Duke Microarray Core Facility. DEG were identified by using the Partek Flow and Partek Genome Suite statistical analysis software (Partek Incorporated). For this, raw data from the 12 hybridizations were imported to Partek Flow for alignment and quality controls. Aligned reads were quantified to transcriptome, filtered out on low expression and normalized. Feature gene lists with DEG were generated and exported to Partek Genome Suite for statistical analysis using ANOVA with multiple test correction. P value lower than 0.05 was established for significance. For Gene ontology (GO), gene symbols of each gene-set were used as input data. The parameters were set as follows: assessment was set to overrepresentation, statistical test to binomial test, multiple testing correction to FWER correction, significance level to 0.05. Among GO evidence codes, inferred from electronically annotated were discarded. The most significant pathway was predicted by considering the selected GO terms and visualized output.

Transfection of plasmids, siRNA and transduction of adenovirus.

For plasmid transfection, primary human TM cells were plated at 80% confluence on 6-well plates in 2 mL of the growth media. Five microgram of the plasmids were dissolved in 167 μ l of 0.3 M CaCl₂. The DNA/ CaCl₂ mixtures were then added dropwise to equal volume of 2xHBS (280 mM NaCl, 1.5 mM Na₂HPO₄, 50 mM HEPES [MilliporeSigma, H0887]) and mixed gently by repeated pipetting. DNA/CaCl₂/HBS suspensions were immediately added to the cells also in a dropwise fashion while gently swirling the plate, and cells were returned to the incubator for 6 h. The DNA-calcium phosphate precipitates were then removed by incubating the cells in a medium pre-equilibrated in a 10% CO₂ for approximately 30 min and replaced with original growth medium. Cells were incubated at 37°C, 5% CO₂ for 48 h for plasmid expression. For

siRNAs transfection, a total of either 5 pmol of siRNA against PKD2 (siPKD2, sc-40863), SMAD2/3 (siSMAD2/3, sc-37238), AKT1 (siAKT1, sc-29195) or 5 pmol of non-targeting siRNA (siNC, sc-37007) were transfected. All siRNAs were obtained from Santa Cruz Biotechnology.

Immunocytochemical analyses

Human TM cells fixed with 4% paraformaldehyde/PBS for 15 min at room temperature. After washing three times with PBS, the cells were incubated in blocking solution (1% Goat Serum [MilliporeSigma, G9023], and 0.1% Triton X-100 [MilliporeSigma, Tx1568-1] in PBS) at room temperature for 30 min. Cells were then incubated for 1 h at room temperature with primary antibodies diluted in blocking solution, washed several times with PBS, and incubated for 1 h at room temperature with Alexa Fluor 488 or 594 dye-conjugated goat anti-mouse or rabbit IgG antibodies (Invitrogen, A-11032 or A-11037) diluted 1:1000 in blocking solution. The cells were subsequently washed with PBS and counterstained with DAPI (1 µg/ml; Thermo Fisher Scientific, 62248). Primary antibodies and dilutions used in this study were: anti-acetylated TUBA4A (1:2000; MilliporeSigma, T7451), anti-IFT88 (1:1000, ProteinTech, 13967-1-AP), anti-SMO (1:500; a gift from Prof. Matthew P. Scott, Stanford University), anti-TGFβ R-I (1:500, EMD Millipore, ABF17-I) and TGFβ R-II (1:500, Cell signalling Technology, 79424S), anti-LC3 (1:1,000, MBL, PM036) anti-Atg16L (1:1,000, MBL, PM040), anti-γ-TUB (1:500, MilliporeSigma, T6557).

Trabecular meshwork tissue flat mounts

The anterior segments of the eye were fixed with 4% paraformaldehyde/PBS overnight and TM tissues were dissected. The tissues were then washed three times for 10 min in 0.5% Triton-X100 in PBS at room temperature and permeabilized overnight in permeabilized buffer (2% Triton-X100 in PBS) at 4°C with agitation. TM tissues were subsequently incubated for 3 days at 4°C with anti-acetylated TUBA4A (1:1,000 in 2% Triton-X100 /2% normal goat serum in PBS). After a series of washes in permeabilization buffer, TM tissues were incubated at room temperature for 4 h with Alexa Fluor 594 dye-conjugated goat anti-mouse IgG antibodies (1:500 in permeabilization buffer). Nuclei were counterstained with DAPI (1 µg/ml in 0.5% Triton-X100 in PBS) for 30 min at room temperature. Samples were then washed in 0.5% Triton-X100 in PBS three times, mounted in Fluoromount-G aqueous mounting media (Thermo Fisher Scientific, 00-4958-02) and coverslipped.

Whole cell lysate preparation and western blot analysis.

Whole cell lysates were prepared by lysing the cells for 30 min on ice with a modified RIPA lysis buffer (MilliporeSigma, R0278) containing 1:100 Halt protease and phosphatase inhibitor cocktail (Thermo Fisher Scientific, 78842). Protein concentration was quantified using a protein assay kit (Micro BCA; Thermo Scientific, 23235). For WB analysis, proteins (2.5-10 µg) were separated by SDS-PAGE (10-15%) and transferred to PVDF membrane. After blocking with 5% non-fat dry milk in PBS-T (0.1% Tween-20) for 1 h, the PVDF membrane was incubated with primary antibodies for overnight at 4°C. Membrane was washed three times with PBS-T and incubated with peroxidase-conjugated secondary antibodies for 1 h at room temperature. Signal was detected by using enhanced chemiluminescence substrate system. The images were captured and quantified by using ChemiDoc™ Touching Image system with Image Lab™ touch software (Bio-Rad, Hercules, CA, USA). The primary antibodies and dilutions used in this study were: anti-LC3B antibody (1:3,000; Cell Signaling Technology, 3868S), anti-SQSTM1 antibody (1:5,000; MilliporeSigma, P0067), anti-SMAD2/3 antibody (1:2000, Cell Signaling, 3102S), anti-phospho-SMAD2/3 antibody (S465,467/ S423,425; 1:2000, Cell signaling Technology, 8828S), anti-phospho-SMAD3 antibody (S423/425; 1:2000, Cell signaling Technology, 9520T), anti-AKT1 antibody (1:2000, Cell signaling

Technology, 9272S), anti-phospho-AKT1 antibody (S473; 1:2000, Cell signaling Technology, 4060S), anti-PKD2 antibody (1:1,000; Santa Cruz Biotechnology, SC-47734) and anti-ACTB antibody (1:1,000; Santa Cruz Biotechnology, SC-69879). Band densities were obtained with Image Lab™ software and normalized with that of ACTB.

Pig eye dissection and perfusion for Outflow facility measurement in porcine anterior segments.

Porcine eyes (4 pairs) were enucleated at Neese Country Sausage (Burlington, NC), delivered in a moist chamber at 4°C within 6 h of death and dissected within 10 h of death. The eyes were sterilized by dipping into 5% betadine/DPBS for 5 min and then transferred into sterile DPBS after removal of excessive external structures such as eyelids and surrounding connective tissue. In a tissue culture hood, the eyes were hemisected at the equator and the vitreous and lens were removed. The ciliary processes were carefully dissected out, with frequent rinsing to remove pigment. The iris was trimmed from the root and then the pectinate ligaments were carefully detached. The ciliary muscle and conventional outflow pathway tissues were left intact and the anterior segments were mounted into perfusion chambers. Anterior segment chambers were maintained at 37°C, 5% CO₂. A syringe pump (PHD 2000 Programmable Syringe Pump, Harvard Apparatus, Holliston, MA, USA) and a pressure transducer (Pressure Sensor 142PC01G, Honeywell, Golden Valley, MN, USA) were used to generate a constant inflow rate or measure intra-chamber pressure, respectively.

Histology

Perfused anterior segments of pig eyes were fixed for 24 h in a 2% paraformaldehyde, 2.5% glutaraldehyde in 0.1 M cacodylate buffer (pH 7.2), washed in 1xPBS and post-fixed for 90 min in 1% OsO₄ in 1xPBS. Complete dehydration was achieved using an increasing ethanol gradient ending in two cycles of propylene oxide. Tissue was infiltrated by immersion in successive propylene oxide:EMbed-812 (1:1, 1:2, 1:3) mixtures and pure EMbed-812 (Electron Microscopy Sciences, Item #14120). A final EMbed-812 immersion was subjected to a vacuum for 4–10 h. Tissue was then transferred to labeled molds pre-filled with degassed EMbed-812 and cured at 20 °C for 24-48 h. Sections were cut to 300 nm thickness using an EM UC7 Ultramicrotome (Leica Microsystems, Wetzlar, Germany) and diamond knife and contrast stained with 1% methylene blue, 1% sodium borate. Images were taken by CELENA® X High Content Imaging System (Logos biosystems, Annandale, VA, USA).

Fig. S1. Identification of differentially expressed genes in autophagy-deficient TM cells under CMS. **(A)** Schematic diagram for microarray analysis. **(B)** Venn diagram summarizing microarray data analysis.

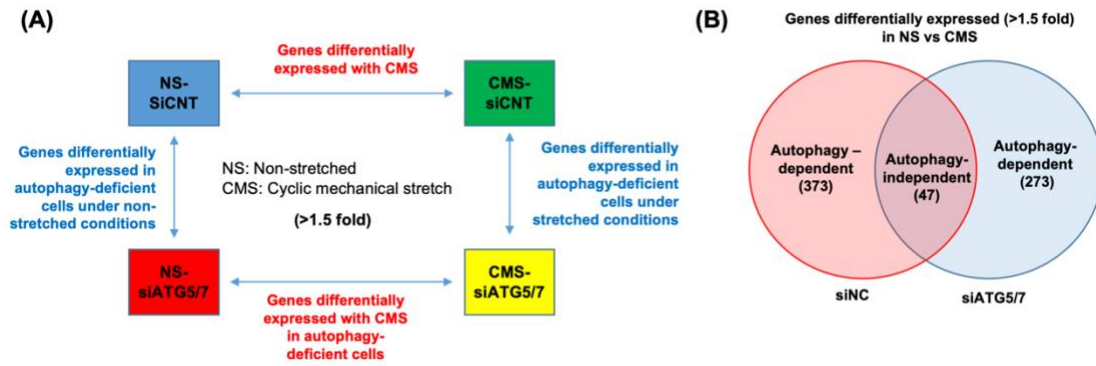


Fig. S2. IFT20 or IFT88 knockdown is not sufficient to prevent CMS-induced autophagy. **(A)** Effect of IFT20 and IFT88 KD on CMS-induced autophagy. TM cells were transfected with siRNA to silence expression of IFT20 (siIFT20) or IFT88 (siIFT88). Induction of autophagy by CMS was tested by monitoring LC3-II levels by WB. Graph shows quantification of densitometric analysis of the bands. Data are shown as the mean \pm S.D. (n=3). *ns*, not significant (Student's *t*-test). **(B)** Representative immunostaining image of primary cilia in siIFT20 and siIFT88-transfected cells. Note that great portion of intact cilia is still observed.

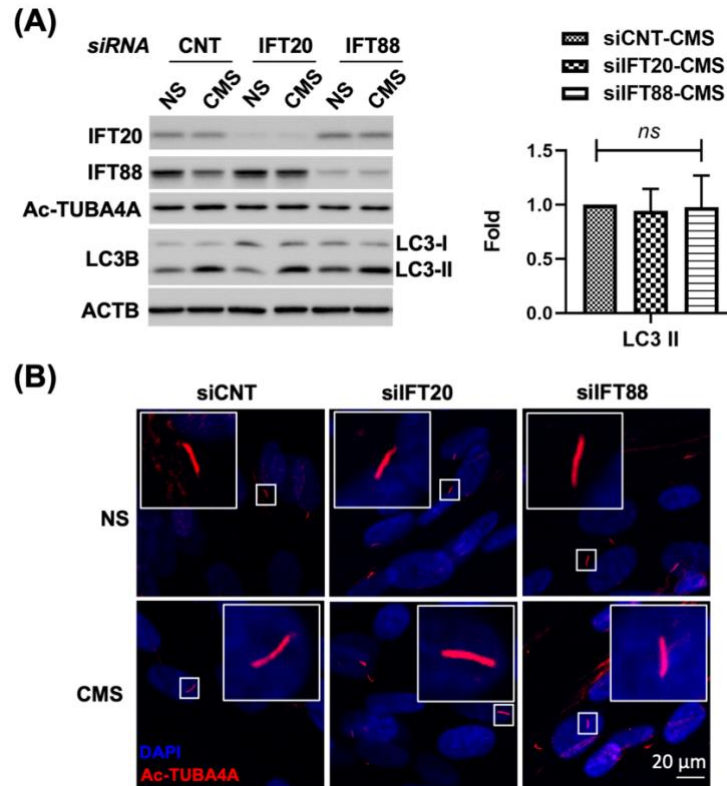


Fig. S3. CMS-induced autophagy is not mediated by Hh/SMO signaling pathway at the primary cilium of TM cells. **(A)** SAG-mediated SMO translocation to the primary cilium. NIH3T3 (positive control) and TM cells were treated with SAG (100 nM) for 4 h, fixed and immunostained with specific antibodies against SMO (green) together with acetylated TUBA4A (red). DAPI was used to stain nuclei. In agreement with the previous report [1], Stimulation with SAG clearly resulted in the enrichment of endogenous SMO into the primary cilium in TM cells as well as NIH3T3 cells (white arrow, inset). **(B)** Representative immunocytochemical analyses of SMO translocation to the primary cilium in TM cells subjected to CMS for 24 h. Note that in contrast to that reported for starvation, CMS did not trigger translocation of SMO to the cilia. **(C)** Effect of cyclopamine on CMS-induced autophagy. TM cells were treated with cyclopamine (2.5–10 μ M), a Hh signaling antagonist, as indicated in Methods. Expression levels of LC3 were measured in whole cell lysates by WB. LC3-II band intensities were normalized by ACTB and fold changes calculated and graphed. Data are shown as the mean \pm S.D. (n =3). *ns*, not significant (ANOVA). Cyclopamine did not significantly prevent the increase in LC3-II levels by CMS in TM cells.

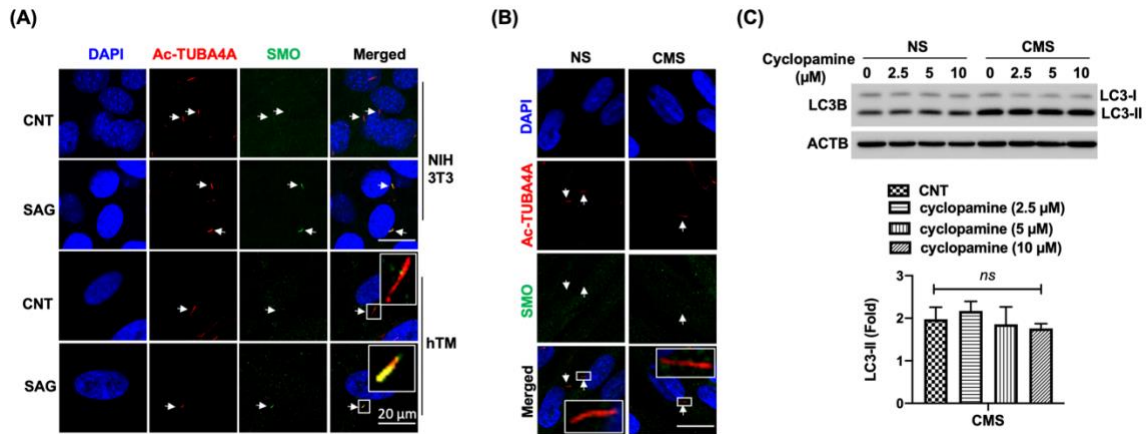


Fig. S4. LKB1 KD does not prevent CMS-induced autophagy. Autophagy induction by CMS were tested in TM cells depleted LKB1. Note that LKB1 KD did not reduce the increased LC3-II level by CMS. ACTB was used as a loading control.

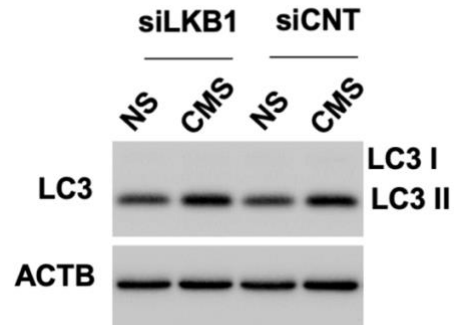


Fig. S5. CMS-induced autophagy is not regulated by canonical TGF β /SMAD signaling pathway. **(A)** Dynasore treatment prevents DQ-BSA endocytosis. Cyan signals indicate fluorescent peptides released by proteolytic degradation of DQ-BSA after endocytosis by TM cells. Note that the signals are reduced by dynasore treatment at a concentration 200 μ M. **(B)** Effect of dynasore on LC3-II levels measured by WB. **(C)** Effect of TGF β R₁ inhibition on TGF β -2-mediated SMAD2/3 phosphorylation in TM cells. Cells were pre-treated 2 h with 10 μ M LY2109761 and SB431542, following by 15 min with TGF β -2 (10 ng/ml); pSmad2/3 phosphorylation levels were evaluated by WB. **(D)** Measurement of autophagy induction in SB431542-treated cells. GFP-LC3 puncta were observed in AdGFP-LC3-transduced TM cells treated with SB431542 (10 μ M) for 24 h. GFP-LC3 puncta are indicated by arrows in each inset of representative images in left panel. The graph represents the quantification of GFP-LC3 puncta. Data are shown as the mean \pm S.D. (n=6). ***, p<0.001 (two-tailed unpaired Student's *t*-test). **(E)** Representative WB blot analysis of SMAD2/3 phosphorylation upon CMS (15 min and 1 h). Treatment with TGF β -2 (10 ng/ml, 15 min) was used as control.

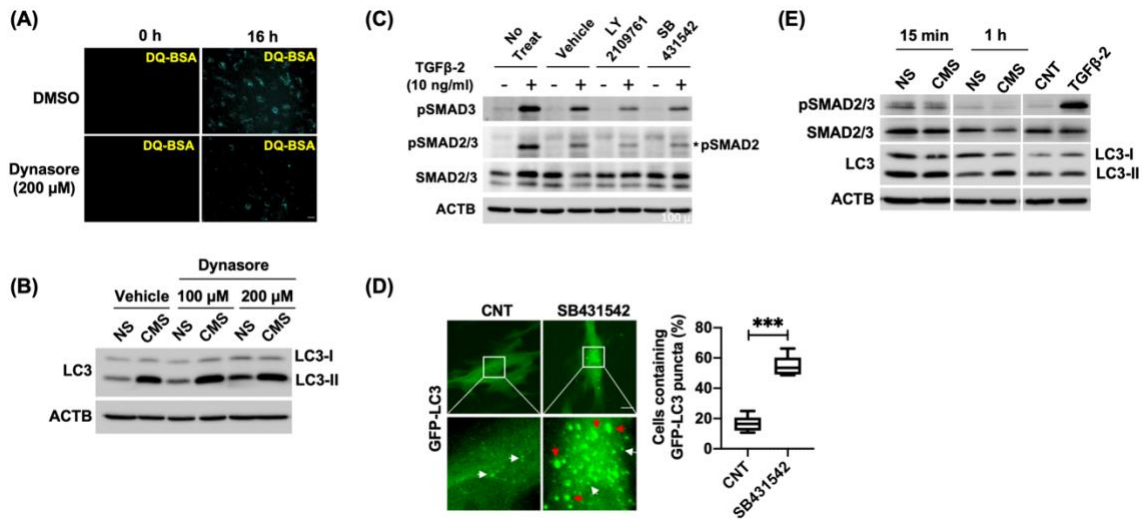


Fig. S6. Representative sagittal thick sections from perfused eyes showing integrity of the TM structures. AAP: the angular aqueous plexus.

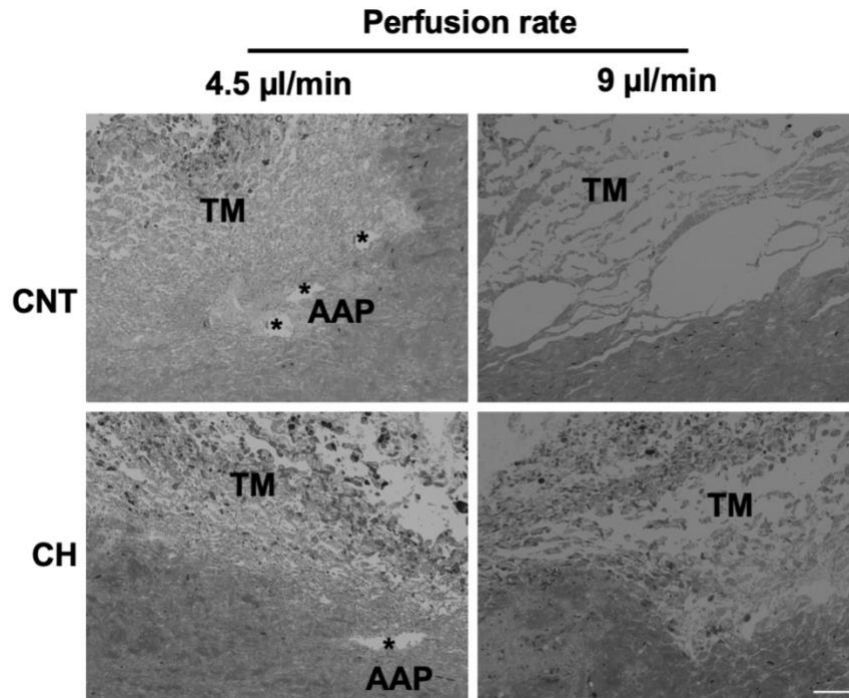


Fig. S7. AKT1-SMAD2/3 crosstalk regulates CMS-induced autophagy in primary human fibroblast cells. Autophagy induction, SMAD2/3 and pAKT1/AKT1 levels were tested in the fibroblast cells depleted SMAD2/3 or AKT1 with or without CMS (n=1 due to the cell availability). Note that SMAD2/3 or AKT1 knockdown shows the similar pattern as shown in TM cells. ACTB was used as a loading control.

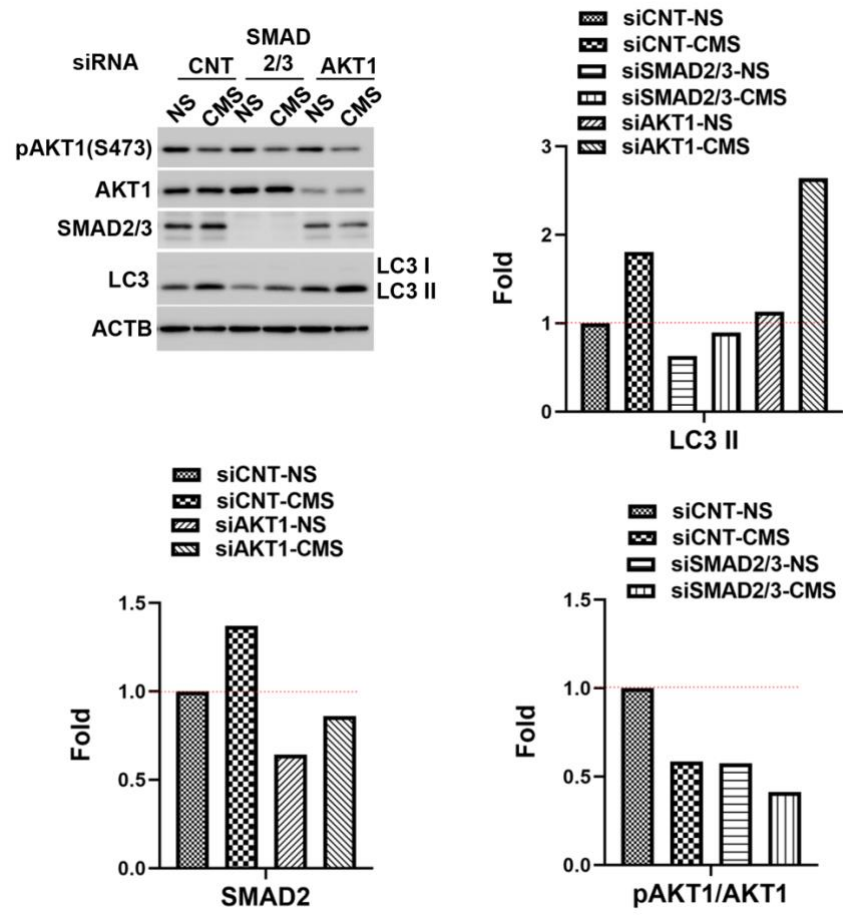


Table S1. List of biological process over-represented in autophagy deficient cells subjected to CMS.

Gene set	Biological process	Corrected p-value	Genes
Up (4)	Metabolic process		
	Cholesterol biosynthetic process	1.66E-07	ID11 FDPS NSDHL EBP CYP51A1 HMGCR FDFT1
	Isoprenoid biosynthetic process	1.84E-03	ID11 FDPS HMGCR FDFT1
	Cellular nitrogen compound biosynthetic process	2.42E-02	MOS DTYMK AD11 NME7 DDAH2 PHGDH ATP1B3 DBI GLUL
	Organelle organization		
	Nucleosome assembly	1.84E-02	HIST1H2BO HIST1H2BJ HIST1H2BK HIST1H4I HIST2H2BE
Down (8)	Transcriptional process		
	Positive regulation of transcription from RNA polymerase II promoter	8.56E-03	MKL2 IL11 MAML2 PLAGL1 LIF INHBA
	Secretion process		
	Negative regulation of hormone secretion	8.56E-03	IL11 LIF INHBA
	Progesterone secretion	4.59E-02	INHBA
	Signaling pathway		
	Positive regulation of peptidyl-serine phosphorylation	3.74E-02	IL11 LIF
	Cell surface receptor linked signaling pathway	4.09E-02	PTGER4 GPR39 CXCL12 MAML2 LIF STC1 INHBA
	Development and differentiation process		
	Regulation of macrophage differentiation	3.29E-02	LIF INHBA
	Eyelid development in camera-type eye	4.59E-02	INHBA
	Positive regulation of myeloid cell differentiation	4.59E-02	LIF INHBA
Up (10)	Cell cycle process		
	Mitotic spindle elongation	4.27E-05	PRC1 KIF23
	Positive regulation of exit from mitosis	4.27E-05	UBE2C BIRC5
	Mitotic chromosome movement towards spindle pole	4.27E-05	CENPE DLGAP5
	Phosphoinositide-mediated signaling	4.47E-05	SPAG5 UBE2C TYMS AURKA
	Positive regulation of ubiquitin-protein ligase activity involved in mitotic cell cycle	8.37E-05	CDC20 CCNB1 UBE2C PLK1
	Mitotic chromosome condensation and metaphase plate congression	1.41E-03	NUSA1 NCAPH CENPE CCNB1
	Anaphase-promoting complex-dependent proteasomal ubiquitin-dependent protein catabolic process	1.77E-03	CDC20 CCNB1 UBE2C
	Positive regulation of mitotic cell cycle	2.59E-03	CCNB1 BIRC5
	G2/M transition of mitotic cell cycle	3.33E-03	CCNB1 BIRC5
Positive regulation of centriole replication	7.75E-03	PLK4	
Down (6)	Metabolic process		
	Steroid metabolic process	3.11E-03	ABCA1 AKR1B10 CYP24A1 FAP ADM CYP17A1
	Heparin biosynthetic process	8.69E-03	ANGPT1 GLCE
	Vascular process in circulatory system	2.17E-02	GCLC ANGPT1 GCLM
	Glutathione biosynthetic process	2.46E-02	GCLC GCLM
	Glutamate metabolic process	4.66E-02	GCLC GCLM
	Quality control		
Regulation of biological quality	4.08E-02	ABCA1 GCLC ANGPT1 FAP BAMBI RDH10 DIO2 ADM S1PR3 GCLM F3	

Movie S1 (separate file). Primary cilium in primary TM cells.

Movie S2 (separate file). Primary cilium dynamics in cultured primary TM cells.

Video S3 (separate file). Effect of CH concentration on TM cell viability.

Video S4 (separate file). Ca²⁺ response upon ionomycin in primary cilia of TM cells.

SI References

1. Rohatgi R, Milenkovic L, Scott MP. Patched1 regulates hedgehog signaling at the primary cilium. *Science* 317, 372-6 (2007).